AJNR

Can Induction of Systemic Hypotension Help Prevent Nidus Rupture Complicating Arteriovenous Malformation Embolization?: Analysis of Underlying Mechanisms Achieved Using a Theoretical Model

Tarik F. Massoud, George J. Hademenos, William L. Young, Erzhen Gao and John Pile-Spellman

AJNR Am J Neuroradiol 2000, 21 (7) 1255-1267
http://www.ajnr.org/content/21/7/1255

AJNR Am J Neuroradiol 21:1255–1267, August 2000

Can Induction of Systemic Hypotension Help Prevent Nidus Rupture Complicating Arteriovenous Malformation Embolization?: Analysis of Underlying Mechanisms Achieved Using a Theoretical Model

Tarik F. Massoud, George J. Hademenos, William L. Young, Erzhen Gao, and John Pile-Spellman

BACKGROUND AND PURPOSE: **Nidus rupture is a serious complication of intracranial arteriovenous malformation (AVM) embolotherapy, but its pathogenetic mechanisms are not well described. An AVM model based on electrical network analysis was used to investigate theoretically the potential role of hemodynamic perturbations for elevating the risk of nidus vessel rupture (R_{rupt}) after simulated AVM embolotherapy, and to assess the potential benefit of systemic hypotension for preventing rupture.**

METHODS: **Five separate hypothetical mechanisms for nidus hemorrhage were studied: 1) intranidal rerouting of blood pressure; 2) extranidal rerouting of blood pressure; 3) occlusion of draining veins with glue; 4) delayed thrombosis of draining veins; and 5) excessively high injection pressures proximal to the nidus. Simulated occlusion of vessels or elevated injection pressures were implemented into the AVM model, and electrical circuit analysis revealed the consequent changes in intranidal flow, pressure, and R_{rupt} for the nidus vessels. An expression for R_{rupt} was derived based on the functional distribution of the critical radii of component vessels. If AVM rupture was observed ($R_{rupt} \geq 100\%$) at systemic normotension (mean pressure [P] = 74 mm Hg), the theoretical embolization was repeated under systemic hypotension (minor P = 70 mm Hg, moderate P = 50 mm Hg, or profound P = 25 mm Hg) to assess the potential benefit of this maneuver in reducing hemorrhage rates.**

RESULTS: **All five pathogenetic mechanisms under investigation were able to produce rupture of AVMs during or after embolotherapy. These different mechanisms had in common the capability of generating surges in intranidal hemodynamic parameters resulting in nidus vessel rupture. The theoretical induction of systemic hypotension during and after treatment was shown to be of significant benefit in attenuating these surges and reducing R_{rupt} to safer levels below 100%.**

CONCLUSION: **The induction of systemic hypotension during and after AVM embolization would appear theoretically to be of potential use in preventing iatrogenic nidus hemorrhage. The described AVM model should serve as a useful research tool for further theoretical investigations of AVM embolotherapy and its hemodynamic sequelae.**

Considerable strides have been made in the field of endovascular embolotherapy of intracranial arteriovenous malformations (AVMs) since the first embolization procedure was reported in 1960 (1). Notwithstanding this evolution, the embolization of AVMs, as currently practiced, continues to carry a significant intrinsic risk of transient or permanent neurologic deficits or death (2). The complication of intracranial hemorrhage remains the most life-threatening sequela of intracranial AVM embolization (2). In a series of 283 AVMs treated with embolotherapy, periembolization subarachnoid hemorrhage and intracerebral hemorrhage occurred in 3.1% and 2.1% of patients, respectively (2).

To date, little attention has been paid to the pathogenetic mechanisms that result in the occurrence of nidus rupture in association with AVM embolotherapy (3). No prior reports exist that specifically investigate the mechanisms responsible for these iatrogenic events. A better understanding of

Received June 16, 1999; accepted after revision February 7, 2000.

From the Division of Interventional Neuroradiology and Department of Radiological Sciences (T.F.M., G.J.H.), University of California at Los Angeles School of Medicine, Los Angeles; Departments of Radiology (T.F.M., W.L.Y., J.P.-S.), Anesthesiology (W.L.Y.), and Neurological Surgery (W.L.Y., J.P.-S.), College of Physicians and Surgeons, and the Department of Electrical Engineering (E.G.), Columbia University, New York, New York.

This study was supported by National Institutes of Health grant RO1 HL/NS52352.

Address reprint requests to Tarik F. Massoud, MD, Section of Neuroradiology, University Department of Radiology, Cambridge University School of Clinical Medicine, Addenbrooke's Hospital, Box 219, Hills Road, Cambridge C82 2QQ U.K.

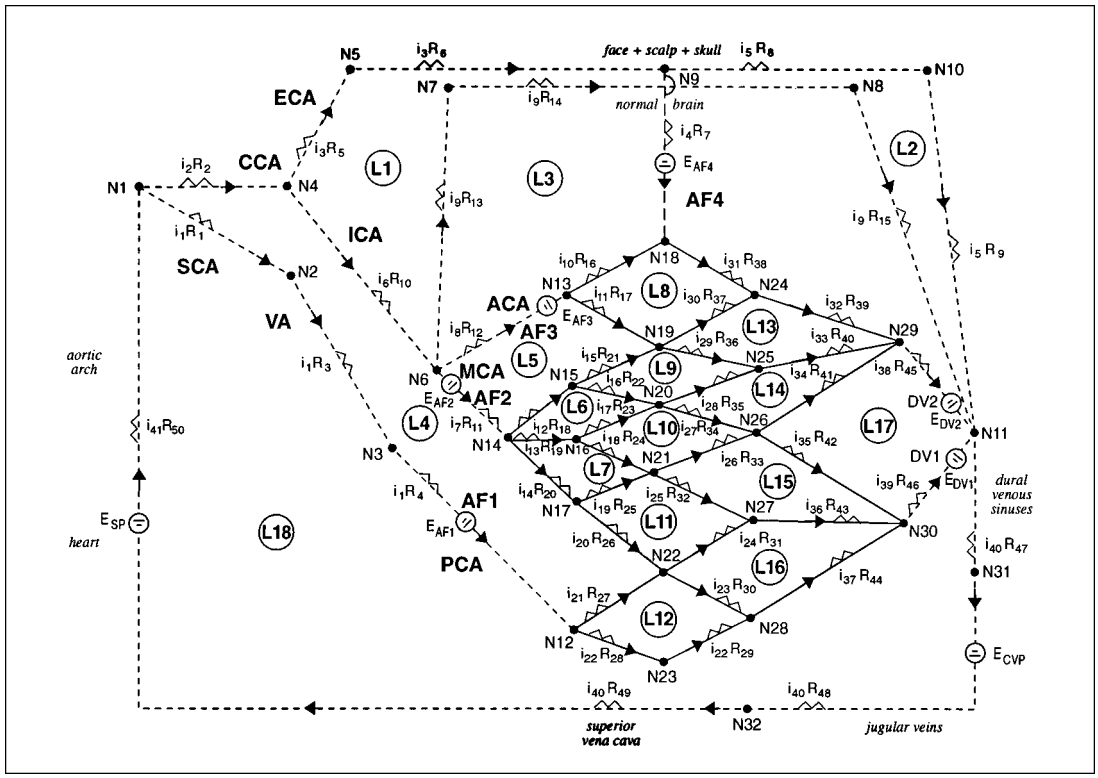

FIG 1. Schematic diagram of the electrical network describing the biomathematical AVM hemodynamic model. CCA, common carotid artery; ECA, external carotid artery; ICA, internal carotid artery; SCA, subclavian artery; VA, vertebral artery; PCA, posterior cerebral artery; ACA, anterior cerebral artery; MCA, middle cerebral artery; E, electromotive force; N, node; L, loop; i, blood flow; R, resistance; SP, systemic pressure, AF, arterial feeder; DV, draining vein; CVP, central venous pressure. (Reproduced with permission of authors and publisher, reference 4).

the underlying hemodynamic and biophysical mechanisms implicated in altering the risk of AVM nidus rupture with embolization is required. This may help to define further those extrinsic contributing factors (for example, those related to the embolization technique or strategy that is used, or those determined by the skill of the operator) and intrinsic contributing factors (that may be related to the characteristics of the AVM being treated) that must be taken into consideration to reduce/eliminate iatrogenic hemorrhagic complications. Ultimately, this knowledge may help in lowering the morbidity and mortality for patients treated by embolization.

A detailed study of events occurring within an AVM nidus, prior to and during its endovascular occlusion with embolic agents, has been hampered by the usual inherent angioarchitectural complexities of these lesions, and the lack of sufficient resolution with current imaging techniques to enable the acquisition of detailed intranidal fine structural or hemodynamic information or both. Furthermore, the lack of possible microcatheter access to minute and fragile plexiform vessels precludes a direct comprehensive appraisal of intranidal hemodynamics.

The recent development and applicability of biomathematical models as experimental investigative tools in the field of cerebrovascular therapy (4–6) helps somewhat to overcome this limitation in that they provide at least the theoretical means to investigate intranidal AVM hemodynamics on a qualitative basis. A biomathematical AVM model was developed previously based on electrical network analysis and possessing a multiple array of simulated intertwining plexiform and fistulous nidus vessels (4). In the present study, this AVM model was used to test the theoretical frameworks and legitimacy of five different mechanisms that have been speculated upon previously in the literature as possible mechanisms for nidus rupture complicating AVM embolotherapy. In addition, a more important goal was to test the theoretical benefit of induced systemic hypotension as a way to reduce elevated risks of nidus rupture during and after AVM embolotherapy.

Methods

The details of this AVM model and its calculations are described elsewhere (4–6), in the Appendix and in Figure 1.

Simulations of AVM Embolization

The described model was used to simulate theoretically the response of an intracranial AVM to transarterial embolizations. Of note, the model used was a representation of a single AVM. Ideally, a large spectrum of computationally and labor-intensive models with varying features and characteristics (6) would have been used to simulate a multitude of AVMs and their responses to embolization. The great advantage of using one

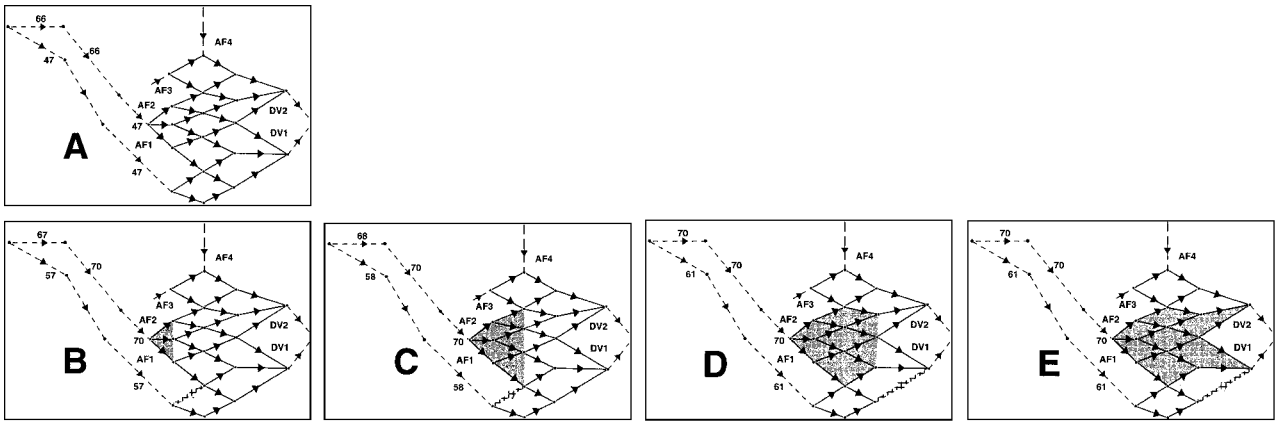

FIG 2. Schematic diagram of a portion of the electrical network AVM model to show the effects of extranidal rerouting of blood pressure after incomplete nidus occlusion with embolic glue (mechanism 2). Panel *A*: Features of the normal AVM model prior to simulated embolization. Note normal mean pressures in vessels i7 (47 mm Hg), i6 (66 mm Hg), i2 (66 mm Hg), and i1 (47 mm Hg) that form a loop outside the nidus. Panels *B* to *E*: Progressive partial occlusion of the nidus with simulated glue (gray) when embolization is achieved via AF2. Note changes in values of mean pressures in the extranidal loop and resulting rupture of nidus vessel i21 (checkered vessel in *B* and *C*) and nidus vessel i37 (checkered vessel in *D* and *E*).

model only, however, is the ability to compare different mechanisms of nidus rupture in a simulated single AVM.

Five mechanisms (numbered 1 to 5) of nidus rupture were investigated; the first four of these by the application of different patterns or schemes of AVM vessel occlusion. These first four modeled patterns were based on clinical knowledge derived from: 1) previously reported hypotheses as to how AVMs might rupture after embolic agent deposition in the nidus (3, 7); 2) previously reported angiographic observations of the various patterns by which vessels of an AVM nidus tend to occlude owing to the spread and deposition of embolic glue (8, 9); and 3) previously documented iatrogenic complications due to the spread of embolic glue or thrombus to AVM draining veins (10). The fifth mechanism of nidus rupture was studied by subjecting the AVM nidus vessels to simulated surges in intravascular pressure caused by elevated injection pressures originating more proximally within the arterial feeders. These five possible mechanisms of nidus rupture and the corresponding categories of AVM embolization simulations that form the central theme of this investigation are outlined in more detail in the following sections.

Intranidal Rerouting of Blood Flow.—It has been suggested by Viñuela et al (11) that abrupt embolic occlusion of an intranidal fistula may result in rerouting of significantly high shunting blood flow through delicate plexiform portions of a nidus, which may result in their immediate rupture. This speculative mechanism of intranidal redistribution of hemodynamic forces was tested in the AVM model by occlusion of the four intranidal fistulous vessels in a systematic fashion, individually and in all possible combinations that included adjoining fistulous vessels (while maintaining all plexiform vessels patent). The minimum number of occluded fistulous vessels was one, and the maximum number was all four in continuity. Thus, a total of 10 experimental simulations of AVM embolotherapy were possible, reflecting occlusion of the intranidal fistula to varying degrees (Table 1). For each simulation, the blood flow, intravascular pressure, and risk of rupture were calculated for all remaining unoccluded nidus vessels (see Appendix).

Because it is believed that intranidal fistulous vessels carry higher hemodynamic loads than their plexiform counterparts (12), it was reasoned, in conceiving the above schemes of vessel occlusion, that if dangerous rerouting of flow and intravascular pressure were to occur, then this would be more likely consequent to redistribution from the fistulous to the weaker and narrower plexiform vessels, and not vice versa. However, to scrutinize the hemodynamic significance and consequences (with regard to nidus rupture) of occluding intranidal fistulous vis-à-vis plexiform vessels further, three additional sets of 10 experimental simulations were performed as control experiments to the first set described above by occluding similar combinations of: 1) four (ie, a similar number to the fistulous vessels) random plexiform vessels (i11, i12, i26, and i32—chosen through use of a random number generator) while maintaining the intranidal fistula patent; 2) the four random plexiform vessels in addition to occluding the four fistulous vessels (Table 1); and 3) the four vessels i13, i18, i25, and i36 (originally fistulous in nature) that were rendered deliberately into plexiform instead (ie, in an entirely plexiform nidus).

Extranidal Rerouting of Blood Flow.—A likely mechanism of postembolization nidus rupture has been pointed out previously by Kvam et al (13), and subsequently emphasized by Spetzler et al (14, 15), and others (3, 16). This results from partial nidus embolization causing upstream pressure elevations in arterial feeders; this pressure increase is subsequently rerouted extranidally and transmitted to persistently unobliterated portions of the nidus, contributing to peri- or postembolization AVM rupture. This mechanism was tested in the AVM model by progressive occlusion of the nidus emanating from the site of ingress of AF2 (as if embolic glue were being injected via AF2) and spreading toward the draining veins (Fig 2) in a manner compatible with clinical observations by Dion and Mathis (8). Accompanying this simulated nidus occlusion, it was assumed that the resulting intravascular pressure within AF2 (vessel i7) would rise (as has been shown previously in experimental and clinical settings [17]) to the maximum extent possible, because the distal aspect of this feeder and its junction with the nidus was assumed to be always totally occluded by the simulated embolic glue. This maximum pressure would have to be no more than the surrounding normal cortical arterial pressures; ie, approximately 90% to 95% of mean systemic pressure. This value is 70 mm Hg in our model. Once these two prerequisites (the schemes of increasing nidus obliteration and a resulting mean pressure of 70 mm Hg in AF2) were determined, AVM model simulations were performed to establish two factors: 1) intranidal rupture occurs in the persistently patent aspects of the nidus as it progressively undergoes embolization via AF2, and 2) the corresponding rises in intravascular pressure in extranidal vessels i6, i2, and i1 (Fig 1 and 2). These particular extranidal vessels are connected to the nidus in the form of a loop and, therefore, form a potential route for transmission of the elevated pressure in AF2 (ie, 70 mm Hg) back to patent aspects of the nidus via an alternative feeder (AF1). Any rises in pressure within these vessels might suggest the occurrence of extranidal rerouting of he-

TABLE 1: Results of theoretical simulations of intranidal rerouting of blood flow consequent to partial embolization of the AVM (mechanism 1)

Occluded Fistulous Nidus Vessel	Occluded Plexiform Nidus Vessels (i_{11}, i_{12}, i_{26}, i_{32})	Nidus Vessel Demonstrating Rupture	Value of Risk of Rupture (%) for Ruptured Nidus Vessel when Embolization Performed at Systemic:		
			Normotension	Moderate Hypotension	Profound Hypotension
(A) Occlusion of Intranidal Pistulous Vessels Only					
i_{13}	· · ·	none	· · ·	· · ·	· · ·
$i_{13} + i_{18}$	· · ·	none	· · ·	· · ·	· · ·
$i_{13} + i_{18} + i_{25}$	· · ·	none	· · ·	· · ·	· · ·
$i_{13} + i_{18} + i_{25} + i_{36}$	· · ·	none	· · ·	· · ·	· · ·
i_{18}	· · ·	none	· · ·	· · ·	· · ·
$i_{18} + i_{25}$	· · ·	none	· · ·	· · ·	· · ·
$i_{18} + i_{25} + i_{36}$	· · ·	none	· · ·	· · ·	· · ·
i_{25}	· · ·	i_{24}	100.5	86.4	62.8
		and i_{26}	100.8	86.7	63.2
$i_{25} + i_{36}$	· · ·	i_{26}	101.3	87.2	63.7
i_{36}	· · ·	i_{26}	100.9	86.9	63.4
		and i_{37}	100.5	86.4	62.9
(B) Occlusion of Intranidal Fistulous and Plexiform Vessels					
i_{13}	√	none	· · ·	· · ·	· · ·
$i_{13} + i_{18}$	√	none	· · ·	· · ·	· · ·
$i_{13} + i_{18} + i_{25}$	√	none	· · ·	· · ·	· · ·
$i_{13} + i_{18} + i_{25} + i_{36}$	√	none	· · ·	· · ·	· · ·
i_{18}	√	none	· · ·	· · ·	· · ·
$i_{18} + i_{25}$	√	none	· · ·	· · ·	· · ·
$i_{18} + i_{25} + i_{36}$	√	none	· · ·	· · ·	· · ·
i_{25}	√	i_{17}	100.5	86.4	62.9
		and i_{24}	101.1	87.0	63.4
$i_{25} + i_{36}$	√	i_{17}	100.8	86.8	63.2
		and i_{37}	100.0	85.9	62.4
i_{36}	√	i_{17}	100.6	86.6	63.0

Note.—For position of individual nidus vessels, see Figure 1. The values of risk of rupture for individual AVM nidus vessels in their normal state prior to embolization ranged from 4.4% to 91.2%. A value of risk of rupture >100% implied nidus vessel rupture. All nidus vessels not experiencing rupture had risk values <100%.

modynamic forces and implicate this in the production of nidus rupture.

Extension of Embolic Glue to Draining Veins.—The disastrous complication that occurs when embolic glue extends to and undergoes polymerization within draining veins, resulting in immediate rupture of an AVM nidus (9, 10), was simulated by occluding DV1 totally in the presence of varying degrees of distal intranidal fistula occlusion. These schemes of vascular occlusion were conceived in order to simulate the inadvertent extension of glue from the distal intranidal fistula to the main draining vein of the AVM during its embolization. Four simulations in total were performed (Table 2). For each simulation, the blood flow, pressure, and risk of rupture were calculated for all remaining unoccluded nidus vessels, as described previously.

Stasis and Delayed Thrombosis in Draining Veins.—Flow reduction and delayed thrombosis of draining veins (in the absence of glue polymerization in the draining veins) sufficient to induce venous outlet obstruction after partial AVM occlusion has been implicated as a further mechanism for AVM rupture complicating embolization (3, 9, 11, 18). A number of patterns of vascular occlusion of the AVM model were conceived to reflect varying extents of nidus (both plexiform and fistulous portions) embolization and draining vein occlusion that in combination might result in nidus rupture. This produced a total of 15 AVM model simulations, as outlined in Table 3. It can be seen from Table 3 that an attempt was made to represent partial embolization of AVMs by progressively increasing extents (percentages) of nidus vessel occlusion. Owing to the presence of a fistula in this AVM, however, it was reasoned that embolic glue would fill this path of least resistance preferentially, resulting in a non-uniform occlusion of the nidus. Therefore, simulations were performed in such a manner that simulated embolic glue would always occlude the distal third of the fistula to the same extent (percentage) as the more proximal third of plexiform vessels within the nidus (Table 3). It was also argued that stasis and thrombosis of DV1 (that draining the fistula) would be much more significant than that of DV2 consequent to the occlusion of the distal portions of the intranidal fistula. Therefore, this simulated occlusion of the draining veins was weighted toward DV1, with thrombosis of DV2 only occurring once 50% of DV1 had thrombosed. For each simulation, the blood flow, intravascular pressure, and risk of rupture were calculated for all remaining unoccluded vessels of the nidus, as described previously.

Elevated Transarterial Injection Pressures.—High surges in intranidal pressure as a result of the dissipation of elevated downstream arterial feeder injection pressures (during delivery of contrast medium or embolic agents or both) may result in AVM nidus rupture (7). This was simulated in the AVM model by increasing the intravascular pressures of AF1 or AF2 by increments of 5 mm Hg to a maximum of 50 mm Hg above baseline intravascular pressure for these feeders. These rises in pressure are typical of those obtained in vessels of experimental animals (19). The resulting AVM simulation, following each distinct increase in arterial feeder pressure, provided values for the blood flow, intravascular pressure, and risk of rupture for all intranidal vessels situated downstream from the site of injection. Twenty-two simulations (11 simulations by simulating injection through AF1 and 11 simulations by injection

TABLE 2: Results of theoretical simulations of embolic glue extension from the intranidal fistula to the draining veins of the AVM (mechanism 3)

Occluded Fistulous Nidus Vessel	Occluded Draining Vein (DV1)	Nidus Vessel Demonstrating Rupture	Value of Risk of Rupture (%) for Ruptured Nidus Vessel when Embolization Performed at Systemic:		
			Normotension	Moderate Hypotension	Profound Hypotension
$i_{13} + i_{18} + i_{25} + i_{36}$	√	none	. . .	. . .	. . .
$i_{18} + i_{25} + i_{36}$	√	none	. . .	. . .	. . .
$i_{25} + i_{36}$	√	i_{34}	103.5	89.5	65.9
i_{36}	√	i_{34}	103.5	89.5	65.9

Note.—For position of individual nidus vessels, see Figure 1. The values of risk of rupture for individual AVM nidus vessels in their normal state prior to embolization ranged from 4.4% to 91.2%. A value of risk of rupture >100% implies nidus vessel rupture. All nidus vessels not experiencing rupture had risk values <100%.

through AF2) were performed at these higher arterial feeder pressures.

Effects of Systemic Hypotension on Risk of Nidus Rupture

In this study, we hypothesized that the induction of systemic hypotension during and after AVM embolization might theoretically be of benefit in reducing the risk of rupture of intranidal vessels by lowering their intravascular pressure and consequent biomechanical stresses on the vessel walls. The previously described mechanisms of AVM rupture consequent to embolization were divided into those that might yield immediate rupture during (or within a few hours of) the procedure (mechanisms 1, 2, 3, and 5), and that which might be delayed, possibly occurring up to weeks after the procedure (mechanism 4). For simulations that yielded cases of immediate rupture during embolization, theoretical systemic hypotension was induced into the AVM circuit by reducing the mean systemic blood pressure from its normal level of 74 mm Hg (4) down to 50 mm Hg (moderate hypotension) or 25 mm Hg (profound/extreme hypotension), as may be possible for short durations in clinical practice using controlled hypotensive anesthesia (20) (vide infra). For simulations that yielded cases of delayed rupture after embolization, theoretical systemic hypotension was induced by a simulated reduction down to 70 mm Hg (minor hypotension), as may be possible in clinical practice using oral antihypertensive medication (21) (vide infra). The resultant reduction in values of mean blood pressure transmitted to the arterial feeders, the draining veins, and the central venous pressure are shown in Figure 3. Therefore, the specific simulations that demonstrated rupture of intranidal vessels at systemic normotension were repeated using these newer levels of lower blood pressure implemented into the AVM circuit. Special attention was paid to any reduction in the value of the risk of rupture with induced systemic hypotension for those vessels that had previously demonstrated rupture at normotension. More specifically, we examined whether systemic hypotension resulted in a risk of rupture $< 100\%$ for nidus vessels with a previous risk $\geq 100\%$.

Results

The simulated total volumetric blood flow through the normal AVM model before any treatment was 814 mL/min, akin to values of flow through large intracranial AVMs (22). The values of risk of rupture for individual AVM nidus vessels in their normal state prior to embolization ranged from 4.4% to 91.2%.

The results of simulating intranidal rerouting of blood flow (mechanism 1) consequent to embolization are shown in Table 1. Nidus rupture (risk of rupture $\geq 100\%$) only occurred with occlusion of the distal aspects of the intranidal fistula (section [A] of Table 1). Occlusion of both fistulous and plexiform vessels did not affect this tendency for rupture to be dictated by occlusion of the distal portions of the intranidal fistula (section [B] of Table 1). No rupture occurred when only four plexiform vessels were occluded nor when vessels i13, i18, i25, and i36 were occluded in an entirely plexiform low-flow (total flow = 234 mL/min) nidus.

The results of simulating extranidal rerouting of blood flow (mechanism 2) consequent to embolization are shown in Figure 2. The baseline intravascular pressures for vessels i7, i6, i2, and i1 prior to nidus embolization are depicted in panel *A*. Progressive nidus embolization and the changes in intravascular pressure in the extranidal loop of vessels under examination is depicted in panels *B–E*. It can be seen that intranidal rupture occurs in the unobliterated portions of the nidus (vessels i21 and i37) fed by AF1. Furthermore, this rupture occurs in conjunction with a redistribution of intravascular pressures in vessels situated extranidally, suggesting that elevations in arterial feeder pressure with partial nidus embolization can be transmitted via other feeders (or branches of the same feeder) to vulnerable patent portions of the nidus. In our model, a mean pressure of 70 mm Hg in AF2 consequent to partial intranidal embolization resulted in a rerouting of blood flow and elevation of AF1 pressure from its normal 47 mm Hg to a maximum of 61 mm Hg. Because of these findings, a further test was performed to examine whether the intranidal rupture occurring in these simulations was a result of extranidal rerouting of blood flow (as suspected), or instead, possibly as a result of an intranidal rerouting of blood flow consequent to the presence of glue within the nidus (ie, as might occur by mechanism 1). Thus, all the described intranidal partial embolization simulations were repeated while preventing AF1 pressure from rising above its normal value of 47 mm Hg (by repeatedly adjusting its resistance). This maneuver eliminated the effects of extranidal rerouting of flow onto the patent portions of the nidus fed by AF1. Should rupture have occurred at this stage, then this might

TABLE 3: Results of theoretical simulations of partial nidus occlusion and delayed thrombosis of AVM draining veins (mechanism 4)

Percentage Occlusion of Plexiform Vessels Located in the:			Percentage Occlusion of Fistulous Vessels Located in the:			Percentage Occlusion of:		Nidus Vessel Demonstrating Rupture	Value of Risk of Rupture (%) for Ruptured Nidus Vessel at Systemic:	
Proximal ⅓ of Nidus	Middle ⅓ of Nidus	Distal ⅓ of Nidus	Proximal ⅓ of Nidus	Middle ⅓ of Nidus	Distal ⅓ of Nidus	DV1	DV2		Normotension	Minor Hypotension
25	0	0	0	0	25	0	0	none	· · ·	· · ·
25	0	0	0	0	25	25	0	none	· · ·	· · ·
25	0	0	0	0	25	50	0	none	· · ·	· · ·
25	0	0	0	0	25	75	25	none	· · ·	· · ·
25	**0**	**0**	**0**	**0**	**25**	**100**	**50**	**i_{34}**	**102.7**	**97.6**
50	25	0	0	25	50	0	0	none	· · ·	· · ·
50	25	0	0	25	50	25	0	none	· · ·	· · ·
50	25	0	0	25	50	50	0	none	· · ·	· · ·
50	25	0	0	25	50	75	25	none	· · ·	· · ·
50	25	0	0	25	50	100	50	none	· · ·	· · ·
75	50	25	25	50	75	0	0	none	· · ·	· · ·
75	50	25	25	50	75	25	0	none	· · ·	· · ·
75	50	25	25	50	75	50	0	none	· · ·	· · ·
75	50	25	25	50	75	75	25	none	· · ·	· · ·
75	50	25	25	50	75	100	50	none	· · ·	· · ·

Note.—For position of individual nidus vessels, see Figure 1. The values of risk of rupture for individual AVM nidus vessels in their normal state prio r to embolization ranged from 4.4% to 91.2%. A value of risk of rupture >100% implies nidus vessel rupture. All nidus vessels not experiencing rupture had risk values <100%.

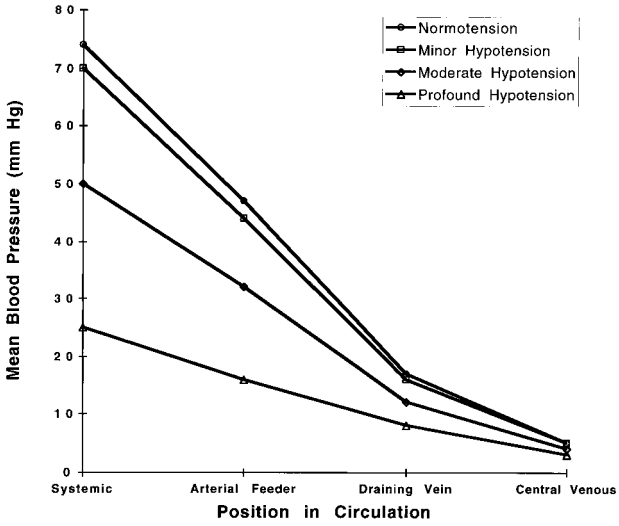

FIG 3. Line diagram representing mean blood pressure drops across the theoretical AVM according to position within the circulation. At normotension, mean systemic pressure is 74 mm Hg. When systemic hypotension is induced in the circulation, the mean systemic pressure falls to 70 mm Hg (minor hypotension), 50 mm Hg (moderate hypotension), or 25 mm Hg (profound hypotension).

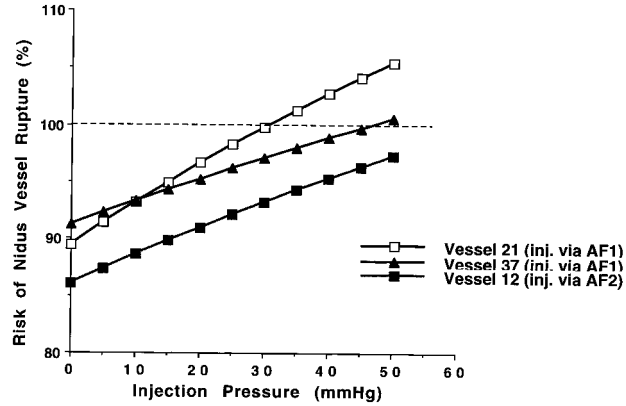

FIG 4. Graph to show how injection pressures (that are in addition to the baseline intravascular pressures) in intranidal vessels i21 and i37 (when an injection is performed through AF1), and in vessel i12 (when an injection is performed through AF2) affect the risk of rupture of these vessels. Vessels i21 and i37 rupture (risk >100%) with high injection pressures.

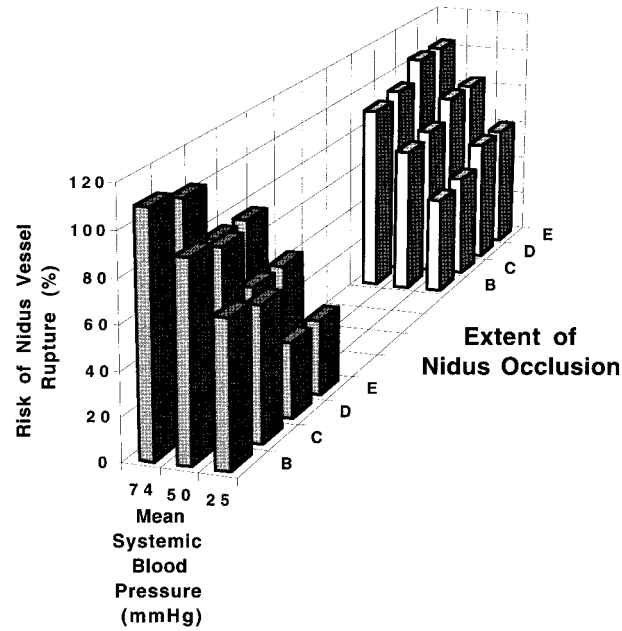

FIG 5. 3D bar chart to show changes in risk of rupture for intranidal vessels i21 (*dark columns*) and i37 (*light columns*), both of which were found to rupture after extranidal rerouting of pressure consequent to partial embolization via AF1 (mechanism 2, as in Fig 2). *B* to *E* represent extent of progressive nidus occlusion as depicted in Figure 2. Note that both vessels rupture (risk >100%) at systemic normotension (74 mm Hg). The reduction in risk of rupture occurs with moderate systemic hypotension (50 mm Hg) and is more pronounced at profound systemic hypotension (25 mm Hg).

have suggested that intranidal (not extranidal) rerouting of flow was the main culprit in the generation of nidus rupture. Our results, however, showed that rupture did not occur when maintaining AF1 pressure at 47 mm Hg, pointing to extranidal rerouting of blood flow as the likely main cause of the observed rupture in patent aspects of the nidus.

The results of simulating extension of embolic glue to the draining veins of an AVM (mechanism 3) are shown in Table 2. Nidus rupture was observed when occlusion of the distal aspects of the intranidal fistula occurred in conjunction with obstruction of DV1.

The results of simulating blood stasis and eventual delayed thrombosis in the draining veins of an AVM (mechanism 4) are shown in Table 3. Nidus rupture was observed when a small extent of the nidus was obliterated in conjunction with considerable thrombosis of both draining veins.

The results of simulating the effects of elevated injection pressures within arterial feeders (mechanism 5) on the risk of rupture in downstream intranidal vessels are shown in Figure 4. Pressure increases in AF1 resulted in rupture of two intranidal vessels (i21 and i37), whereas simulated injections through AF2 only resulted in a marked rise in risk of rupture for vessel i12, but actual rupture did not occur.

Theoretical systemic hypotension was investigated in all cases of AVM nidus rupture that were observed during the study of mechanisms 1 to 5. For all cases of nidus rupture observed at systemic normotension, the repetition of the same simulated embolization in the presence of systemic hypotension resulted in a lowering of the risk of nidus rupture to <100%. This observed theoretical benefit during or after embolization was present with all three degrees (minor, moderate, and profound) of systemic hypotension. The extent by which the risk of nidus rupture was reduced appeared proportional to the degree of systemic hypotension—the greatest reduction in risk of nidus rupture occurred during profound systemic hypotension. This is exemplified and illustrated in Figure 5, which demonstrates

graphically the reduction in risk of rupture for intranidal vessels i21 and i37, both of which were found to rupture after extranidal rerouting of pressure consequent to embolization via AF1 (as explained above for mechanism 2; also see Figure 2).

Discussion

Causes of Embolotherapy-induced Hemorrhage

Other than the five possible mechanisms of nidus rupture complicating AVM embolotherapy that form the subject of our present theoretical study, there exist several other potential causes of intracranial hemorrhage consequent to AVM embolization that cannot be investigated with this particular AVM model. The most important of these causes is rupture of dysplastic aneurysms situated within an AVM nidus or more proximally on arterial feeders (7, 8, 23). These aneurysms occur in up to 58% of AVMs (24), and have a significant impact on the strategies adopted to induce embolization in these AVMs in an effort to avoid aneurysm rupture during the procedure. Analysis of the theoretical hemodynamic alterations present within an aneurysm subsequent to partial embolization of an AVM requires an overall more complex theoretical modeling process (which takes into account a combination of AVM and aneurysm models), and, therefore, will be the subject of a separate future study. Four other suggested causes of intracranial hemorrhage that may complicate embolization of AVMs, but that were not investigated in this study, are: 1) the ''normal perfusion pressure breakthrough'' phenomenon (13, 16, 25–27); 2) ''occlusive hyperemia'' (28, 29); 3) potential direct toxicity of embolic agents on nidus vessel walls (30–32); and 4) recanalization of previously occluded nidus portions that results in reexposure of blood flow to weakened vessel walls (33). Also, other mechanical causes of rupture and hemorrhage that specifically affect arterial feeders (23, 34), such as traumatic microcatheter or microguidewire manipulations, were not simulated in this study.

Biomathematical AVM Model

Models are necessary to achieve reproducibility, which is an essential component of scientific experimentation (35). The numerous advantages of biomathematical modeling and the rationale behind using this experimental approach have been described previously (4, 36). Biomathematical models offer one way to understand theoretically AVM physiologic mechanisms under normal hemodynamic conditions and during simulated therapy, particularly in a region of an AVM (the nidus) that is otherwise inaccessible to detailed investigations by any other current technique. Generally speaking, the results of biomathematical modeling are not intended to be extrapolated directly to the clinical setting but, instead, to be used as a framework within which clinical phenomena can be better understood and possible implications suggested, and as a forum for research and exploration of new ideas (37). The advantages and disadvantages of the specific AVM model used in this study have been discussed at length previously (4–6). Extrapolation to a human AVM setting may not be possible with this model in assessing the risk of hemorrhage after treatment, but qualitative appreciation can be obtained for the ability of embolization to induce hemodynamic and biomechanical alterations in the stability of the nidus vessels and to induce rupture.

The general principles and philosophical premises of modeling in biomedical research have been reviewed in detail by the authors recently (38); the current modeling study was conducted within the framework of these previously reported guidelines. It bears reiterating that a large potential for error exists when adopting this research approach. Limitations of the modeling process as applied to biomedical systems in general include:

1. The process is subjective. For example, in the current study numerous assumptions were made in model creation and in the ensuing embolization simulations (as described in the Methods section). Small errors in any of these assumptions have the potential for causing large errors in experimental results. Dedicated parameter sensitivity analysis studies are necessary to establish the extent of any such error.
2. Models represent isolated systems, whereas the real systems being modeled are rarely isolated, or even isolatable in principle.
3. Minimal-parameter models may not be explanatory to one's satisfaction because they may neglect properties that are emphasized in more traditional physiologic work. Thus it may be necessary to ''overmodel'' in the mathematical sense, to provide a model that has appeal to a community of scholars who have arrived at their understandings of the real world (e.g. of AVMs) through a different route.
4. A serious pitfall arises when the results of modeling experiments, such as this one, are believed to be entirely descriptive of the real-world situation (ie, embolization of AVMs) rather than realizing that they are merely the implications of the hypothesis built into the model. Regardless of how carefully created or complete a theoretical analysis may be, there always remains the danger that such scientific extrapolation may be logical but not at all descriptive of the real world. Until actual measured data from human AVMs back up theoretical predictions, these predictions remain in the world of uncertainty. Therefore, the purpose of the experimental approach adopted in this study is to provoke contemplation and reflection upon the issues presented, and not to take place of new experimental observations.

Mechanisms of Nidus Rupture at Embolotherapy

It has long been speculated that hemodynamic disturbances resulting from embolization of AVMs might be responsible for iatrogenic hemorrhagic complications. These hemodynamic disturbances may take on two forms that act independently or in association: 1) an elevation of intravascular pressure proximal to the site of an obstruction, and 2) a rerouting of blood flow and pressure away from the site of an obstruction.

No direct evidence exists to support the notion that intranidal rerouting of dangerous hemodynamics from one part of the nidus to another can cause AVM rupture. Instead, on empirical grounds it has been believed by Viñuela et al (11), and alluded to earlier by Kvam et al (13), that such rerouting does occur locally within an AVM nidus. Our results lend theoretical support to this potential mechanism of nidus rupture, especially when an intranidal fistula is obstructed.

Contrary to the mechanism of intranidal rerouting of hemodynamics at AVM embolization, that occurring extranidally is publicized much more often as a probable mechanism of AVM hemorrhage (3, 13–15). The occurrence of extranidal rerouting of blood flow via sperate feeders can be appreciated readily on transcranial Doppler studies during and after AVM embolization (39). Moreover, it is known for certain that downstream obstruction within the AVM circulation (eg, by partial embolization of the nidus) causes more proximal elevations in intravascular pressure within arterial feeders (14, 15, 17, 40). It is then assumed that these higher intravascular pressures are or can be transmitted back (rerouted) to patent aspects of the nidus, causing them to rupture. This, however, has never been demonstrated by simultaneous measurements of intravascular pressure in separate feeders (as compared with the transcranial Doppler study referenced previously). The results of this study indicate that these assumptions appear well founded, at least from a theoretical standpoint. In the AVM model used, partial embolization was capable of inducing extranidal elevations in pressure that were relayed back (via a different feeder) to unoccluded parts of the nidus resulting in their rupture.

The evidence that partial nidus embolization causes more proximal elevation of pressure within arterial feeders has been described by Gao et al (41). A downstream obstruction within the nidus exerts an equal yet opposite force against the hemodynamic forces generated by blood pressure within the arterial feeder in driving the blood through the nidus. Therefore, the pressure level at the site of the obstruction builds up (and is transmitted upstream) to become equal in magnitude to that at the source of the pressure head (ie, that driving the previously patent arterial feeder). This elevated pressure in an obstructed feeder can: 1) be transmitted back to the nidus via the same feeder (if this is partially occluded) or alternative branches/feeders (3, 13–16); 2) result in progressive dilatation of the stagnant feeder and even its eventual rupture (13, 27) or rupture of an associated dysplastic aneurysm (13); 3) be transmitted to adjacent cerebral tissue to result in hyperemic complications (13, 16, 25–27); and/or 4) simply equilibrate with the intravascular pressure in adjacent vessels/vascular beds. For this reason, we postulate that the maximum possible extent to which mean pressure in an obstructed feeder can elevate consequent to nidus embolization is the same value as mean pressures in normal cortical vessels of that patient; ie, about 90% of mean systemic blood pressure. In this regard, Ahuja et al (42) observed postembolization hemorrhages in two patients in whom mean arterial feeder pressures increased to above 80% (reaching $>$85% of mean systemic pressure levels) of the preembolization levels. Also, Handa et al (40) noted that there was a gradual increase in arterial feeder pressure as each subsequent injection of embolic agent occluded greater portions of an AVM nidus. As the arteriovenous shunt decreased, the pressure gradually increased in the arterial feeders, so that well-embolized and poorly embolized AVMs had mean feeder pressure increases of 27 mm Hg and 11 mm Hg, respectively.

The complication of draining vein occlusion with embolic glue is a dreaded one because it can lead to immediate (10) or delayed (27) AVM rupture. Our results lend support to this mechanism. Embolization of a draining vein, however, does not always lead to complications (43). In one series, glue underwent polymerization within AVM draining veins in seven patients, no clinical sequelae ensued in six patients, and in one patient nidus rupture occurred 12 hours after embolization (44). Based on such findings, it has been speculated that occlusion of the draining vein may or may not be significant, depending on the size and dynamic importance of this vessel and flow changes through the nidus (43). The results of this study concur with these ideas and provide a theoretical backing to this mechanism of nidus rupture following embolization.

When embolization of an AVM nidus is incomplete but is greater than 50% in extent, progressive thrombosis may ensue for at least three reasons (45, 46): 1) reduced intranidal flow, 2) continued thrombogenic effect of the glue, and 3) persistence of the inflammatory process following exposure of nidus vessels to the embolic agent. This progressive thrombosis may lead to two possible changes in the remaining patent aspects of the nidus and in the draining veins. First, it may lead to complete obliteration of the nidus, with or without distal extension to segments of the draining veins (45). Alternatively, the resultant flow stasis predominates, and the progressive thrombosis occurs only/mainly in the draining veins while sparing the residual portions of the AVM nidus. This resultant venous outlet obstruction, occurring in the presence of patent nidus remnants, can lead to rupture (11). Viñuela et al (11) reported on two patients who bled 4 and

5 days post embolization, both of whom had 50% to 75% nidus obliteration, noticeable early stagnation in the draining veins, and no glue or underlying stenoses in the draining veins. Extensive thrombosis of the draining veins was confirmed at surgery for removal of these AVMs.

Injections of excessive volumes of fluid (34) or elevated injection pressures (7, 47) can cause vessel perforation, but this is usually reported in relation to rupture of arterial feeders or associated dysplastic aneurysms or both. For example, Nakstad et al (48) reported rupture of a small arterial branch of a large AVM feeder when injecting 0.5 mL of contrast medium. Rupture of an arterial feeder may also occur because of direct injection pressure in the presence of a partially occluded artery; eg, with embolic particles (7). Our results suggest that this mechanism might also operate within the nidus. Elevated injection pressures (within the ranges simulated in this study) during delivery of contrast medium or embolic agent in arterial feeders could lead to rupture of downstream nidus vessels.

Influence of Systemic Hypotension

Several authors have reported on methods that attempt to reduce the risk of hemorrhage during or immediately after AVM surgery or embolization. Of particular note, these maneuvers are usually driven at lowering the potentially dangerous elevated pressures in arterial feeders of AVMs after partial nidus obliteration. Thus, Spetzler et al (14) have stressed the importance of proximal arterial feeder ligation or clipping after intraoperative nidus embolization. Sorimachi et al (16) have extended the same principle to endovascular procedures by suggesting proximal occlusion of stagnant arterial feeders with coils. Even ligation of the cervical internal carotid artery after AVM embolization has been used in the past (49). Staged embolization or surgery or both of large AVMs is another approach designed to reduce gradually the expected elevations in arterial feeder pressures if a total occlusion/excision of these lesions were to be carried out (8, 14). Interestingly, Tamaki et al (50) have suggested that in these large AVMs it is possible to perform one-stage excision with the aid of graded occlusion of the cervical carotid artery by using Selverstone clamps to ''modulate'' distal blood flow and pressure in the postoperative period.

With regard to induction of systemic hypotension, this has been advocated previously for two reasons in relation to performing endovascular embolization of intracranial AVMs. First, during the procedure, simply as a means to control dynamically the gradual filling of a nidus with slowly polymerizing glue (51); and second, in the immediate period after the procedure, with the patient in intensive care, as a means of reducing possible hyperemic complications (9, 49, 52, 53). There exists a third way to make use of deliberate hypotension as an aid to AVM embolotherapy, but this has been reported on only sparingly (9, 49, 54). To our knowledge, Ling et al (9) are the only group to have reported specifically on the potential benefit of hypotension in lowering the rates of hemorrhage that occurs during AVM embolotherapy. Based on their experience in embolization of 300 AVMs, they recommend a reduction in systemic blood pressure of 20–30 mm Hg from a time just before embolization till the third day post embolization. In this study, we provide a theoretical analysis of the underlying hemodynamic and biophysical mechanisms responsible for a lowering of this risk of AVM rupture with systemic hypotension.

The induction of systemic hypotension (eg, by using the vasodilators sodium nitroprusside, esmolol, or isoflurane alone or in combination [55]) is a routine technique for cerebrovascular surgery (56, 57), and has been employed as well during conventional transarterial embolization of AVMs (51). Mean systemic pressure levels of 40–50 mm Hg are compatible with brain safety because they do not preclude subsequent restoration of mitochondrial redox of cytochrome *a* and *a*3 in cerebral cortical cells, and somatosensory evoked potentials are maintained (20). Profound controlled hypotension, even down to mean systemic pressures of 25 mm Hg, may be tolerated for a limited time (58).

The results of this theoretical study raise the possibility that even moderate systemic hypotension (mean pressure of 50 mm Hg) during embolization of AVMs might be of benefit in maintaining the risk of AVM rupture below dangerously critical levels. This applies to mechanisms 1 to 3 and mechanism 5 in this study, because these mechanisms tend to yield early rupture, and, therefore, the use of hypotensive anesthesia during the embolization might counteract any potential elevations in risk of AVM rupture. Mechanism 4, on the other hand, tends to result in delayed rupture, even up to a month after the embolization (18). Our results suggest that for this duration, even minor reductions in systemic blood pressure might be helpful in avoiding AVM rupture by mechanism 4. In normotensive patients, a minor sustained reduction of systemic blood pressure, eg, by 4–5 mm Hg, is possible with oral antihypertensive medication (21). This degree of hypotension usually has no clinical side effects (21). It is therefore tempting to propose, in partially embolized AVMs in which a prominent degree of stagnation is observed in the draining veins on postembolization angiograms, that these patients might benefit from a short course of oral antihypertensives of a 1-month duration after treatment and after discharge from intensive care. This prophylaxis might prove sufficient to reduce the risk of nidus rupture should delayed venous thrombosis occur.

These suggestions regarding the use of systemic hypotension during and after AVM embolotherapy should be considered within the overall context of this theoretical study. In reality, the inherent biological and biovariability traits of cerebral AVMs

are not accurately or entirely reproducible with a biomathematical model. Thus, it is not possible to simulate complex biological events, nor is it possible to study the impact that heparinization during (3) or after (29) embolization might have on the risk of AVM rupture. Another limitation of the mathematical results of this study is that it is conceptually difficult to judge the real biological impact of minor systemic hypotension on AVM hemodynamics. Given the wide variations in systemic blood pressure experienced during normal activities, and that most AVMs rupture during sleep (59), a reduction of 4–5 mm Hg in mean systemic pressure might appear at first to be insignificant. Of note, Marks et al (53) in a recent small series found no benefit in maintaining the mean systemic pressure at 65–75 mm Hg for 2 to 3 days post embolization.

It remains unclear from this study to what extent these results obtained when using the single AVM model presented could differ in the presence of alternative AVM model hemodynamic features, such as underlying feeder pressure values and total volumetric flow volume. As stated, a large spectrum of computationally and labor-intensive models with varying features and characteristics (as presented in a prior report [6]) would have to be used to simulate a multitude of AVMs and their responses to embolization. This issue was beyond the scope of this study. By future adoption of this approach, we plan to define the sensitivity of the model characteristics to the results of embolization simulations obtained.

The findings of this theoretical study should serve as a springboard for further discussion and analysis of mechanisms of AVM rupture and their prevention. The results of this study can only be verified by further detailed clinical observations following implementation of the suggestions herein on a trial basis, or more ideally, by pooling of data from many centers in a randomized trial to test the benefits of systemic pressure reduction during and after AVM embolization.

Appendix

Electrical Network AVM Model

The AVM network, nestled within a simulated circulatory network of the head and neck, consisted of four arterial feeders, two draining veins, and a nidus angioarchitecture with a randomly distributed array of 28 interconnected plexiform and fistulous components, as shown in Figure 1. Twenty-four of the nidus vessels were plexiform and four nidus vessels were fistulous (i13, i18, i25, and i36 in Figure 1). Two arterial feeders (AF1 and AF2) were considered major feeders, wheras AF3 and AF4 (a simulated transdural supply) were minor feeders. Both draining veins drained into the simulated intracranial venous sinuses.

The pressure values implemented into the AVM circuit were: mean systemic blood pressure of 74 mm Hg; mean arterial feeder pressure of 47 mm Hg (for major arterial feeders); mean arterial feeder pressure of 50 mm Hg (for minor arterial feeders); mean draining vein pressure of 17 mm Hg; and mean central venous pressure of 5 mm Hg. All the above values were considered for the purpose of this study to be ''typical'' or average ones, and were obtained from pooled historical data (4). A separate parameter sensitivity analytical study (6) that characterized the functioning of this AVM model when wide ranges of values (instead of single ones) were implemented into the model, revealed that the adoption of the above values resulted in an acceptable representation of a single ''typical'' high-flow large intracranial AVM based on its total volumetric blood flow rate (814 mL/min) and its baseline risk of rupture (less than 100%).

Using an electrical analogy of Ohm's law, flow rate was determined based on Poiseuille's law given the aforementioned pressures and resistance of each nidus vessel. In order to determine the hemodynamic quantities within each vessel of the vascular array during each simulation of an embolization procedure, network analysis of the loops and nodes constituting the AVM model circuit was performed to yield 41 linear equations corresponding to the 41 vessels of the circuit and yielding 41 distinct values of volumetric flow rate (4). The 41 derived linear equations were solved simultaneously by expanding a simplified version of Poiseuille's formula into matrix form. The matrices corresponding to pressure and resistance were created using a spreadsheet application (Microsoft Excel) and transported to an advanced mathematical computation program (Mathematica, Champaign, IL) for solution of the flow rate values for all 41 vessels (4). Thus, circuit analysis of the AVM vasculature based on the conservation of flow and voltage revealed the flow rate through each vessel in the AVM network. Once the volumetric flow rate was determined for each simulation, it was then possible to calculate other hemodynamic parameters such as the intravascular pressure and the risk of rupture for each nidus vessel.

Risk of AVM Nidus Rupture

The highly tortuous, structurally weak intranidal vessels subjected to the continual impingement of large hemodynamic forces make AVMs highly susceptible to hemorrhage. The precise location or region of rupture is extremely difficult to observe angiographically and to detect histologically, and remains a source of speculation in the study of AVMs. It is believed commonly that, based on the biomechanical properties of the intranidal vessels, rupture occurs when the cumulative hemodynamic stresses of the vessel wall exceeds its elastic modulus (5).

An expression for the risk of rupture can be derived based on the functional distribution of the critical radius over a range of intravascular pressures experienced by a cylindrical vessel during a normal cardiac cycle (5, 6) and is given as: Risk = ln $[P_{exp}/P_{min}]$/ln $[P_{max}/P_{min}]$, where P_{min} and P_{max} are the central venous pressure and the ''maximum intranidal pressure,'' respectively, and P_{exp} is the pressure of the nidus vessel determined during simulation (5, 6). The complete mathematical derivation of the above expression and more detailed discussion of the rationale for the logarithmic expressions and the terms P_{min} and P_{max} are as described in a prior report (5), to which the attention of the reader is directed.

The expression given above represents a relative measurement of the probability or risk of rupture and is multiplied by 100% to present the result as a percentage of risk of rupture. Of particular importance to this study is whether these values of risk of rupture for individual nidus vessels equal or surpass the 100% limit. Should this occur for any nidus vessel, ie, the probability becomes that of certain rupture, then the whole AVM nidus is deemed to have ruptured. The maximum extent to which the risk of rupture rises above 100% is theoretically of no significance—it is merely the occurrence of rupture (ie, the risk being $\geq$100%) that is of paramount importance.

Another method of deriving an expression of risk of nidus vessel rupture has been reported by Gao et al (60). This expression is based on more detailed characteristics of intranidal vessels, and was not used in this study.

References

1. Luessenhop AJ, Spence WT. **Artificial embolization of cerebral arteries: report of use in a case of arteriovenous malformation.** *JAMA* 1960;172:1153–1155
2. Viñuela F. **Functional evaluation and embolization of intracranial arteriovenous malformations.** In: Viñuela F, Halbach VV, Dion JE, eds. *Interventional Neuroradiology: Endovascular Therapy of the Central Nervous System.* New York: Raven Press;1992; 77–86
3. Purdy PD, Batjer HH, Samson D. **Management of hemorrhagic complications from preoperative embolization of arteriovenous malformations.** *J Neurosurg* 1991;74:205–211
4. Hademenos GJ, Massoud TF, Viñuela F. **A biomathematical model of intracranial arteriovenous malformations based on electrical network analysis: theory and hemodynamics.** *Neurosurgery* 1996;38:1005–1015
5. Hademenos GJ, Massoud TF. **Risk of intracranial arteriovenous malformation rupture due to venous drainage impairment: a theoretical analysis.** *Stroke* 1996;27:1072–1083
6. Hademenos GJ, Massoud TF. **An electrical network model of intracranial arteriovenous malformations: analysis of variations in hemodynamic and biophysical parameters.** *Neurol Res* 1996;18:575–589
7. Viñuela F. **Blood pressure monitoring in feeding arteries of cerebral arteriovenous malformations during embolization: a preventive role in hemodynamic complications [Comment].** *Neurosurgery* 1995;37:1047
8. Dion JE, Mathis JM. **Cranial arteriovenous malformations: the role of embolization and stereotactic surgery.** *Neurosurg Clin North Am* 1994;5:459–474
9. Ling F, Bai B, Liu S. **Discussion on the causes of hemorrhage during and after embolization of cerebral AVM.** In: Taki W, Picard L, Kikuchi H, eds. *Advances in Interventional Neuroradiology and Intravascular Neurosurgery.* Amsterdam: Elsevier; 1996;317–320
10. Massoud TF, Duckwiler GR, Viñuela F, Guglielmi G. **Acute subdural hemorrhage complicating embolization of a cerebral arteriovenous malformation.** *AJNR Am J Neuroradiol* 1995;16: 852–856
11. Viñuela F, Dion JE, Duckwiler G, et al. **Combined endovascular embolization and surgery in the management of cerebral arteriovenous malformations: experience with 101 cases.** *J Neurosurg* 1991;75:856–864
12. Yasargil MG. **Pathological considerations.** In: Yasargil MG, ed. *Microneurosurgery IIIA.* Stuttgart: Georg Thieme Verlag;1987; 40–57
13. Kvam DA, Michelsen J, Quest DO. **Intracerebral hemorrhage as a complication of artificial embolization.** *Neurosurgery* 1980; 7:491–494
14. Spetzler RF, Martin NA, Carter LP, Flom RA, Raudzens PA, Wilkinson E. **Surgical management of large AVMs by staged embolization and operative excision.** *J Neurosurg* 1987;67:17–28
15. Spetzler RF, Hargraves RW, McCormick PW, Zabramski JM, Flom RA, Zimmerman RS. **Relationship of perfusion pressure and size to risk of hemorrhage from arteriovenous malformations.** *J Neurosurg* 1992; 76:918–923
16. Sorimachi T, Takeuchi S, Koike T, Minakawa T, Abe H, Tanaka R. **Blood pressure monitoring in feeding arteries of cerebral arteriovenous malformations during embolization: a preventive role in hemodynamic complications.** *Neurosurgery* 1995; 37:1041–1048
17. Duckwiler G, Dion J, Viñuela F. **Intravascular microcatheter pressure monitoring: experimental results and early clinical evaluation.** *AJNR Am J Neuroradiol* 1990;11:169–175
18. Duckwiler GR, Dion JE, Viñuela F, Reichman A. **Delayed venous occlusion following embolotherapy of vascular malformations in the brain.** *AJNR Am J Neuroradiol* 1992;13:1571–1579
19. Saitoh H, Hayakawa K, Nishimura K, et al. **Intracarotid blood pressure changes during contrast medium injection.** *AJNR Am J Neuroradiol* 1996;17:51–54
20. Yamada S, Brauer F, Knierim D, et al. **Safety limits of controlled hypotension in humans.** *Acta Neurochir* 1988;42: (Suppl)14–17
21. Lepor H. **Long-term efficacy and safety of terazosin in patients with benign prostatic hyperplasia.** *Urology* 1995;45:406–413
22. Yamada S, Thio S, Iacono RP, et al. **Total blood flow to arteriovenous malformations.** *Neurol Res* 1993;15:379–383
23. Abe T, Nemoto S, Iwata T, Shimazu M, Matsumoto K, Liu K. **Rupture of a cerebral aneurysm during embolization for a cerebral arteriovenous malformation.** *AJNR Am J Neuroradiol* 1995;16:1818–1820
24. Turjman F, Massoud TF, Viñuela F, Sayre JW, Guglielmi G, Duckwiler G. **Aneurysms related to cerebral arteriovenous malformations: Superselective angiographic assessment in 58 patients.** *AJNR Am J Neuroradiol* 1994;15:1601–1605
25. Deruty R, Pelissou-Guyotat I, Amat D, et al. **Complications after multidisciplinary treatment of cerebral arteriovenous malformations.** *Acta Neurochir* 1996;138:119–131
26. Spetzler RF, Wilson CB, Weinstein P, Mehdorn M, Townsend J, Telles D. **Normal perfusion pressure breakthrough theory.** *Clin Neurosurg* 1978;25:651–672
27. Stein BM. **Surgical decisions in vascular malformations of the brain.** In: Barnett JM, Mohr JP, Stein BM, et al., eds. *Stroke: Pathophysiology, Diagnosis, and Management.* Philadelphia: Churchill Livingstone; 1992;1093–1133
28. Al-Rodhan NRF, Sundt TM, Piepgras DG, Nichols DA, Rufenacht D, Stevens LN. **Occlusive hyperemia: a theory for the hemodynamic complications following resection of intracerebral arteriovenous malformations.** *J Neurosurg* 1993;78:167–175
29. Wilson CB, Hieshima G. **Occlusive hyperemia: a new way to think about an old problem.** *J Neurosurg* 1993;78:165–166
30. Brothers MF, Kaufmann JCE, Fox AJ, Deveikis JP. **N-butyl 2-cyanoacrylate: substitute for IBCA in interventional neuroradiology: histopathologic and polymerization time studies.** *AJNR Am J Neuroradiol* 1989;10:777–786
31. Germano IM, Davis RL, Wilson CB, Hieshima GB. **Histopathological follow-up study of 66 cerebral arteriovenous malformations after therapeutic embolization with polyvinyl alcohol.** *J Neurosurg* 1992;76:607–614
32. Vinters HV, Galil KA, Lundie MJ, Kaufmann JC. **The histotoxicity of cyanoacrylates.** *Neuroradiology* 1985;27:279–291
33. Klara PM, George ED, McDonnell DE, Pevsner PH. **Morphological studies of human arteriovenous malformations: Effects of**

isobutyl 2-cyanoacrylate embolization. *J Neurosurg* 1985;63: 421–425
34. Halbach VV, Higashida RT, Dowd CF, Barnwell SL, Hieshima GB. **Management of vascular perforations that occur during neuro-interventional procedures.** *AJNR Am J Neuroradiol* 1991; 12:319–327
35. Cooper AJ, Johnson CD. **Animal experimentation.** *Br J Surg* 1991;78:1409–1411
36. White R. J, Fitzjerrell DG, Croston RC. **Fundamentals of lumped compartmental modelling of the cardiovascular system.** *Adv Cardiovasc Phys* 1983;5(Part I):162–184
37. Cape EG. **Mathematical modeling in the evaluation and design of surgical procedures.** *J Thorac Cardiovasc Surg* 1996;111: 499–501
38. Massoud TF, Hademenos GJ, Young WL, Gao E, Pile-Spellman J, Viñuela F. **Principles and philosophy of modeling in biomedical research.** *FASEB J* 1998;12:275–285
39. Chioffi F, Pasqualin A, Beltamello A, Da Pian R. **Hemodynamic effects of preoperative embolization in cerebral arteriovenous malformations: Evaluation with transcranial Doppler sonography.** *Neurosurgery* 1992;31:877–885
40. Handa T, Negoro M, Miyachi S, Sugita K. **Evaluation of pressure changes in feeding arteries during embolization of intracerebral arteriovenous malformations.** *J Neurosurg* 1993;79: 383–389
41. Gao E, Young WL, Pile-Spellman J, et al. **Cerebral arteriovenous malformation feeding artery aneurysms: a theoretical model of intravascular pressure changes after treatment.** *Neurosurgery* 1997;41:1345–1356
42. Ahuja A, Gibbons KJ, Guterman LR, Hopkins LN. **Pedicle pressure changes in cerebral arteriovenous malformations during therapeutic embolization: relationship to delayed hemorrhage (abstr).** *Stroke* 1993;24:185
43. Viñuela F, Debrun GM, Fox AJ, Girvin JP, Peerless SJ. **Dominant-hemisphere arteriovenous malformations: therapeutic embolization with isobutyl-2-cyanoacrylate.** *AJNR Am J Neuroradiol* 1983;4:959–966
44. Viñuela F, Fox AJ, Debrun G, Pelz D. **Preembolization superselective angiography: Role in the treatment of brain arteriovenous malformations with isobutyl-2 cyanoacrylate.** *AJNR Am J Neuroradiol* 1984;5:765–769
45. Viñuela F, Fox AJ, Debrun G, Drake CG, Peerless SJ, Girvin JP. **Progressive thrombosis of brain arteriovenous malformations after embolization with isobutyl-2 cyanoacrylate.** *AJNR Am J Neuroradiol* 1983;4:1233–1238
46. Viñuela F, Fox AJ, Pelz D, Debrun G. **Angiographic follow-up of large cerebral AVMs incompletely embolized with isobutyl-2 cyanoacrylate.** *AJNR Am J Neuroradiol* 1986;7:919–925
47. Rauch RA, Viñuela F, Dion J, et al. **Preembolization functional evaluation in brain arteriovenous malformations: the superselective amytal test.** *AJNR Am J Neuroradiol* 1992;13:303–308
48. Nakstad PH, Nornes H. **Superselective angiography, embolization and surgery in treatment of arteriovenous malformations of the brain.** *Neuroradiology* 1994;36:410–413
49. Luessenhop AJ. **Intracerebral hemorrhage as a complication of artificial embolization [Comment].** *Neurosurgery* 1980;7: 493–494
50. Tamaki N, Lin T, Asada M, et al. **Modulation of blood flow following excision of a high-flow cerebral arteriovenous malformation: case report.** *J Neurosurg* 1990;72:509–512
51. Debrun GM, Aletich V, Ausman JI, Charbel F, Dujovny M. **Embolization of the nidus of brain arteriovenous malformations with n-butyl cyanoacrylate.** *Neurosurgery* 1997;40:112–121
52. Lundqvist C, Wikholm G, Svendsen P. **Embolization of cerebral arteriovenous malformations. Part II: Aspects of complications and late outcome.** *Neurosurgery* 1996;39:460–469
53. Marks MP, Norbash AM, Steinberg GK. **Hemorrhagic complications of AVM embolization.** In: Taki W, Picard L, Kikuchi H, eds. *Advances in Interventional Neuroradiology and Intravascular Neurosurgery.* Amsterdam: Elsevier;1996:321–323
54. Wikholm G, Lundqvist C, Svendsen P. **Embolization of cerebral arteriovenous malformations. Part I: Technique, morphology, and complications.** *Neurosurgery* 1996;39:448–459
55. Ornstein E, Young WL, Ostapkovich N, Matteo RS, Diaz J. **Deliberate hypotension in patients with intracranial arteriovenous malformations: esmolol compared with isoflurane and sodium nitroprusside.** *Anesth Analg* 1991;72:639–644
56. Tasman KR. **Anesthetic management of arteriovenous malformation: a case report.** *J AANA* 1996;64:81–88
57. Young WL, Ornstein E. **Perioperative management of high-flow arteriovenous malformations: hemodynamic monitoring and anesthetic considerations.** In: Pasqualin A, Da Pian R, eds. *New Trends in Management of Cerebro-Vascular Malformations.* Vienna: Springer-Verlag;1994;382–389
58. Yamada S. **Arteriovenous malformations in the functional area: surgical treatment and regional cerebral blood flow.** *Neurol Res* 1982;4:283–322
59. Perret G, Nishioka H. **Report on the cooperative study of intracranial aneurysms and subarachnoid hemorrhage.** *J Neurosurg* 1966;25:467–490
60. Gao E, Young WL, Hademenos GJ, **Theoretical modelling of arteriovenous malformation rupture risk: a feasibility and validation study.** *Med Eng Phys* 1998;20:489–501